Lattice modelling of early-age creep of 3D printed segments with the consideration of stress history

Chang, Ze; Liang, Minfei; He, Shan; Schlangen, Erik; Šavija, Branko

DOI
10.1016/j.matdes.2023.112340

Publication date
2023

Document Version
Final published version

Published in
Materials and Design

Citation (APA)
Chang, Z., Liang, M., He, S., Schlangen, E., & Šavija, B. (2023). Lattice modelling of early-age creep of 3D printed segments with the consideration of stress history. *Materials and Design*, *234*, Article 112340. https://doi.org/10.1016/j.matdes.2023.112340

Materials & Design 234 (2023) 112340

Contents lists available at ScienceDirect

Materials & Design

journal homepage: www.elsevier.com/locate/matdes

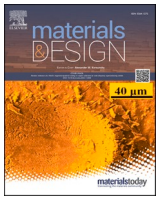

Lattice modelling of early-age creep of 3D printed segments with the consideration of stress history

Ze Chang *, Minfei Liang, Shan He, Erik Schlangen, Branko Šavija

Microlab, Faculty of Civil Engineering and Geosciences, Delft University of Technology, 2628 CN Delft, The Netherlands

ARTICLE INFO

Keywords:
Concrete 3D printing
Lattice model
Early-age creep
Superposition principle

ABSTRACT

We propose a new numerical method to analyze the early-age creep of 3D printed segments with the consideration of stress history. The integral creep strain evaluation formula is first expressed in a summation form using superposition principle. The experimentally derived creep compliance surface is then employed to calculate the creep strain in the lattice model with a combination of stored stress history. These strains are then converted into element forces and applied to the analyzed object. The entire numerical analysis consists of a sequence of linear analyses, and the viscosity is modelled using imposed local forces. The model is based on the incremental algorithm and one of the main advantages is the straightforward implementation of stress history consideration. The creep test with incremental compressive loading is utilized to validate this model. The modelling results are in good agreement with experimental data, demonstrating the feasibility of the lattice model in early-age creep analysis under incremental compressive loading. To understand the impact of early-age creep on structural viscoelastic deformation during the printing process, additional analyses of a printed segment are carried out. These simulation results highlight the need to consider creep for accurate prediction of viscoelastic deformation during the printing process.

1. Introduction

Extrusion-based 3D concrete printing (3DCP) may revolutionize the construction industry through the implementation of construction automation [1–6]. This advanced technology can fabricate the computer-designed geometry of a building in less time than conventional construction, is less labour intensive, and needs a minimum of formwork [2,7].

When it comes to 3D printable cementitious materials, there is a balance between pumpability and buildability [1,7,8]. The former requires that the materials must be sufficiently fluid to be pumped and extruded from the nozzle. The printable materials should be stiff to sustain the geometry under the self-weight and gravitational loading from subsequent printing segments after deposition. In contrast to traditional cementitious materials, the 3D printable concrete/mortar has two characteristic features [9]: (1) viscosity modifying agents (VMAs) are frequently used; (2) high cement content with a low water to cement (w/c) ratio. The first feature enables smooth pumping process without blockage, as it enhances the viscosity of printable materials. The second one allows the extruded materials to be stiff enough, avoiding plastic collapse after material deposition. When these two requirements are satisfied, the cementitious material may be printable.

A price is, however, to be paid for this advantage. Extrusion-based 3D printing may result in increased porosity [10], raising the risk of substantial creep deformation of printed segments. Additionally, a large volume proportion of cement paste produces will result in high creep in concrete, since cement paste is the primary source of creep in concrete [11]. This may impair the durability and long-term serviceability of 3D printed structures. Even though there has been a lot of research on how creep occurs in hardened cementitious materials [6,12–14], an agreement is yet not reached. The viscous characteristics of the hydration products, consisting of portlandite (CH) and calcium-silicate-hydrate (C-S-H), as well as environmental factors, including temperature and relative humidity (RH), all affect creep [14–18].

The viscoelasticity and plasticity become apparent after material deposition, and these material characteristics codetermine structural deformation and failure mode during the printing process. To accurately predict structural deformation and quantify buildability during or after

* Corresponding author.
E-mail addresses: z.chang1006@gmail.com (Z. Chang), M.Liang-1@tudelft.nl (M. Liang), S.He-2@tudelft.nl (S. He), Erik.Schlangen@tudelft.nl (E. Schlangen), B.Savija@tudelft.nl (B. Šavija).

https://doi.org/10.1016/j.matdes.2023.112340
Received 23 September 2022; Received in revised form 26 April 2023; Accepted 19 September 2023
Available online 20 September 2023

printing, it is essential to understand the early-age material behaviour. Several experimental approaches have been proposed for buildability quantification, including the unconfined uniaxial compression test [19], direct shear test [20], rotational rheometer test [21], and ultrasonic wave transmission test [22]. Material properties derived from these experiments, i.e, green strength, yield stress, elastic modulus, viscosity, and others, can be used in numerical or mathematical models for structural analysis of 3DCP [19,23–26]. It should be noted that these material characteristics only consider instantaneous deformation and ignore time-dependent deformation that occurs throughout the printing process. Thus, model predictions may underestimate the structural deformation because time-dependent processes (e.g., creep) are not considered.

Experiments have therefore been conducted to characterize the early-age creep of 3D printable cementitious materials [27–29]. Chen et al. performed rheological tests [28] in which a very small shear force is applied to system to measure the cohesion among dispersed particles within the elastic domain. The formulation of this bond accounts for the colloidal attractive forces induced by the flocculation as well as the chemical reaction due to structuration. Esposito et al. [27], on the other hand, performed uniaxial compressive tests to characterize the early-age creep of 3D printable mortar, in the range of 0 to 60 min. The measured deformation results from different mechanisms: plastic shrinkage, autogenous shrinkage, basic creep, and consolidation settlement under compressive load. The experimental results from uniaxial compression test are comparable to the time-dependent deformation observed during the printing process. To accurately predict structural deformation during or after the printing process, it is crucial to incorporate time-dependent strain into models for structural analysis of 3DCP.

However, to the best of the authors' knowledge, few published model investigates the impact of early-age creep on the prediction of structural deformation of 3DCP. Based on the published research, most creep models are applicable to hardened cementitious materials subjected to constant loading [30–32]. Li et al. [33] proposed a numerical method to explore the early-age viscoelastic behaviour of hydrating cement paste based on the computer-generated microstructural models. Han et al. [34] presented a nonlinear model to predict early-age creep of concrete (about 2 days) subjected to compressive load. However, early-age creep of conventional cementitious materials generally refers to the moment after the final or at least the initial setting time. At that stage, the hydration products grow along with the surface of the cement particles, eventually forming a solid particle skeleton. Creep in the fresh stage (i.e., after casting or deposition from the nozzle in case of extrusion-based 3D printing) has not been considered in the concrete modelling literature.

There are a few possible reasons for this. First, not many experiments focused on early-age creep of 3D printable mortar or concrete. This makes it difficult to calibrate and validate models for early-age creep. Additionally, the continuous printing process causes growth or change of applied stress on printed segments. The complex loading condition poses difficulties in creep simulations due to the stress history. In the finite element method, a Dirichlet series approximation is used to convert continuous compliance functions (i.e., power-law or logarithmic functions) into rate-type laws to predict the creep behaviour of cementitious materials [35,36]. Although creep evolution can be modelled, it is difficult to accurately identify of the numerous empirical parameters needed for the formulation [37]. A creep function with fewer parameters could simplify the computational analysis.

To reduce the number of empirical coefficients needed to define the creep function and make the simulation more straightforward, a lattice-type model is developed herein to simulate the early-age creep of 3D printable mortar. Previously, a 2D lattice model was employed to investigate the effect of microstructure of hardened cement paste on short-term creep behaviour [17]. However, this model does not account for stress history, and cannot therefore be used to simulate creep under variable stress. Further developments of the approach included the incorporation of the effective stress and modulus to account for the elastic and creep components of autogenous shrinkage [38]. Previous research therefore demonstrates the feasibility of lattice model in early-age deformation analysis.

The primary contribution of this study is to propose a numerical method to predict the evolution of early-age creep of 3D printed segments while allowing for stress history of individual elements. The creep analysis consists of a sequence of linear analyses, in which the elastic and creep coefficients are determined based on creep tests. The viscosity is simulated via an imposed local force, which is similar to the effective elastic modulus method proposed by Bažant [15,37,39]. The model is then validated through a series of non-ageing/ageing creep tests.

2. Methodology

2.1. Theoretical background

Laboratory studies of 3DCP demonstrate that the structural deformation of printed segments at fresh stage tends to increase when the gravitational loading is constant. The term "early-age creep" is commonly used to describe this phenomenon.

To describe the early-age creep under incremental compressive loading, stress history must be considered. However, storing the entire stress history will result in a high computational cost and extensive memory use. To address this, methods have been proposed to simplify the computation of creep strain, such as the rate-type creep approach [35,36], effective modulus method [40], ageing coefficient method [41], parallel creep method [42], and others [43]. Using these methodologies, the integral stress–strain relation of creep evolution can be converted into new formulations that only store a limited number of history variables instead of the entire loading history. For instance, the continuous creep function is transformed into a Dirichlet series approximation using the rate-type technique. However, the Dirichlet series expansion involves numerous empirical parameters which are difficult to identify [44].

Herein, a numerical model to predict this delayed deformation during printing process is proposed; it does not distinguish the contribution of influential factors like plastic and autogenous shrinkage as well as consolidation settlement under compressive stress. In contrast to the above-mentioned numerical methods, the proposed method avoids approximating the Boltzmann superposition principle and uses it directly for creep strain calculation. This method avoids the need for fitted parameters, and there is no approximation of the creep constitutive law.

The creep behaviour of cementitious materials can be analyzed using linear viscoelasticity, which enables the consideration of the entire history of stress [37]. To describe the strain evolution with loading time in a creep test, the stress–strain relation can be expressed as

$$\varepsilon(t) = \int_o^t J(t-\tau,\tau)d\sigma(\tau) \tag{1}$$

where the J is the creep compliance function determined by the hardening time (τ) and loading duration (t- τ); σ refers to the stress. The Boltzmann superposition principle is adopted to discretize the integral formulation:

$$\begin{aligned} \varepsilon(t) &= \sum_{i=1}^{i=N} \Delta\sigma(\tau_i) J(t-\tau_i,\tau_i) \\ J(t-\tau_i,\tau_i) &= 1/E(\tau_i) + C_0 C_1(\tau_i) C_2(t-\tau_i) \end{aligned} \tag{2}$$

where $\Delta\sigma$ is the incremental stress; C_0 refers to the creep parameters determined by the material properties and external conditions such as temperature and relative humidity; to ensure the accuracy of C_0, each creep test should be conducted under constant external conditions such as temperature and humidity, and the loading duration is short enough to ensure that the microstructure of the tested sample can be assumed to

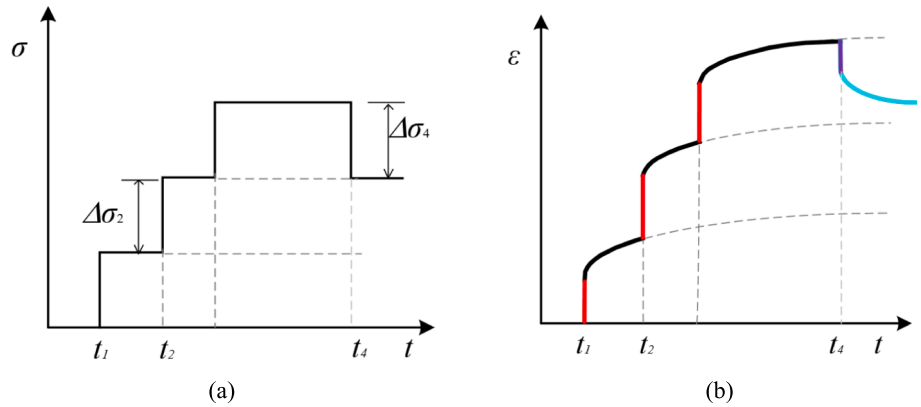

Fig. 1. Schematic diagram of superposition principle (a) piecewise constant stress history with several jumps (b) time-dependent system deformation (adapted from [47]). Red color indicates instantaneous deformation, and black/gray indicate the time-dependend deformation; purple and blue curves refer to the elastic and creep recovery induced by the reduced stress. (For interpretation of the references to color in this figure legend, the reader is referred to the web version of this article.)

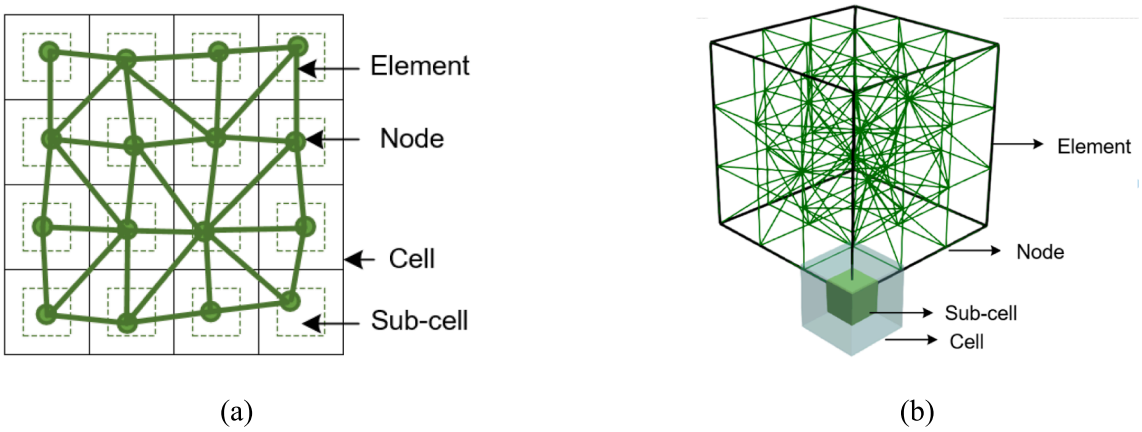

Fig. 2. Schematic diagrams of lattice mesh (a) 2D (b) 3D.

be the same; C_1 is a power function that reflects the impact of hardening/ageing time (τ) on creep compliance; and C_2 is a power function determined by the non-ageing/loading duration (t-τ) [45,46]. The detailed procedure for determining these parameters has been described by Irfan-ul-Hassan et al. [3] and Chang et al. [47]. Irfan ul-Hassan et al. used hourly repeated minute-long quasi-static tests were conducted to determine the elastic and creep properties of young cement paste. They then determined the creep parameters C_0, C_1, and C_2 by fitting the experimental data to a creep model (a power law function).

It must be noted that the Boltzmann superposition is only valid if each period is assumed to be independent. In other words, previous loading steps do not affect the creep response resulting from the applied force at later stages. The superposition principle is valid given that all the principal stresses are below 40–50% of uniaxial strength [48,49]. In that case, the analyzed object is not damaged, and linear viscoelasticity applies [49]. If the stress is higher, a damage law must be incorporated into the numerical model to capture the non-linear creep [37,50]. In this model, the time-dependent material properties are incorporated to account for the effects of curing on material properties, and an element removal mechanism is adopted to mimic the effects of damage. We consider that the change in the material microstructure is small during the short hydration time considered in this study.

The superposition principle allows the loading path to be separated into a sequence of small steps with a time interval of Δt_i, which are independent of each other. In each time interval, the creep force is applied to the tested sample at the onset and remains constant until the end (as shown in Fig. 1 (a)). The final creep evolution is a sum of all the strain curves, as shown in Fig. 1 (b). The total strain of the analyzed object can be computed with the stress history and creep compliance as inputs. For instance, the creep evolution after t_4 in Fig. 1 (b) can be calculated as:

$$\varepsilon(t) = \Delta\sigma_1 J(t - t_{1,}t_1) + \Delta\sigma_2 J(t - t_{2,}t_2) + \Delta\sigma_3 J(t - t_{3,}t_3) + \Delta\sigma_4 J(t - t_{4,}t_4) \tag{3}$$

2.2. Lattice model implementation

The lattice model has been used for fracture and mechanical analysis of disordered heterogeneous materials [51–54]. Wider applications have been carried out over the past decades, including mass transfer [55], corrosion [56], shrinkage [57,58], Alkali-Silica Reaction (ASR) [59], creep analysis [17] and simulation of the concrete 3D printing process [23,24]. In this study, the lattice model is extended to simulate the viscoelasticity of cementitious materials.

Lattice modelling of the early-age creep consists of two components, i.e., the model discretization and creep numerical analysis. The analyzed object is discretized as illustrated in Fig. 2: (a) The continuum is first divided into a network of cells; (b) A sub-cell is defined within each cell; the ratio of the length between sub-cell and cell controls the randomness of the mesh system; (c) Lattice nodes are randomly placed within each sub-cell; (d) Delaunay tessellation is used to connect adjacent nodes to form the lattice beams. The continuum is finally schematized as a set of Timoshenko beams, which can transfer the axial forces, shear forces, bending moments, and torsion.

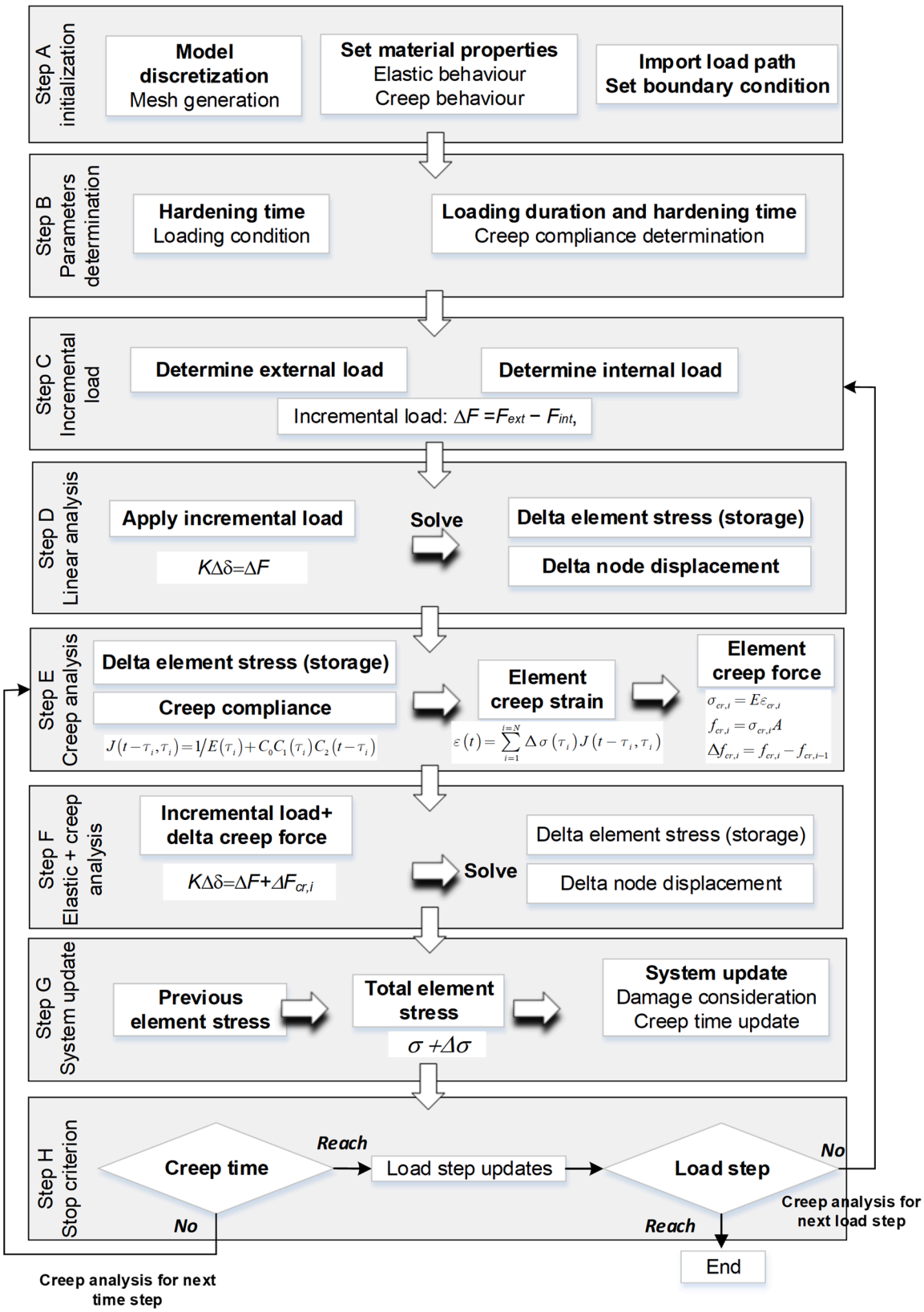

Fig. 3. Flowchart about Lattice model on creep analysis.

2.3. Model implementation

Section 2.1 briefly describes how to compute the creep strain of lattice elements. In this section, these computed strains will be converted into element forces and applied to the elements. This approach is herein termed the 'local force method'. The details pertaining the model implementation are shown in Fig. 3.

This flowchart describes how lattice model simulates the viscoelastic

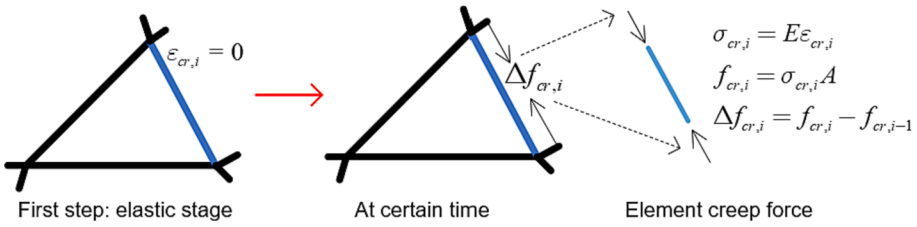

Fig. 4. The creep deformation and local axial force of an individual beam element.

behaviour of 3D printable mortar. This includes 8 steps: A, B, C, D, E, F, G, and H.

Step A: Model discretization

Model discretization has been described in Section 2.2. The relevant material properties are assigned to the beam elements. Besides, the designed load path is imported into the lattice model as the external boundary for creep and fracture analysis.

Step B: Determination of creep parameters

When it comes to the creep analysis, the creep compliance plays a significant role and can be computed with the hardening time and loading duration as inputs. The obtained creep compliance is then incorporated with the superposition principle for the calculation of element creep strain, as expressed by Eq..

Step C: Incremental load

The difference between the external and internal loading is defined as a disequilibrium force in the incremental algorithm, as expressed by Eq.. The former refers to the loading condition imported from the load path, while the latter is computed considering the internal force as well as element orientation.

Step D: Linear analysis

In this step, the governing equation (i.e., Eq) is solved by means of the conjugate gradient method.

$$\begin{aligned} K_e \Delta D &= \Delta F \\ \Delta F &= F_{ex} - F_{in} \end{aligned} \tag{4}$$

Steps E and F: Creep analysis

Given the known creep compliance and obtained incrmental element stress, the creep strain of individual elements can be computed based on Eq.. These element strains are then converted into elemental normal forces. The difference between two steps' creep forces is defined as incremental creep force in each analysis step. These forces are calculated as:

$$\begin{aligned} \sigma_{cr,i} &= E\varepsilon_{cr,i} \\ f_{cr,i} &= \sigma_{cr,i}A \\ \Delta f_{cr,i} &= f_{cr,i} - f_{cr,i-1} \end{aligned} \tag{5}$$

Here, E refers to the elastic modulus of printable mortar and A is the cross-sectional area of a lattice beam. f and σ are element force and stress for creep analysis. This derived incrmental creep force $\Delta f_{cr,i}$ is then applied to the lattice element, as shown in Fig. 4, together with the previously computed disequilibrium force in each step. These applied local forces enable the simulation of time-dependent deformation. Using this method, the entire analysis for viscoelasticity can be conducted by solving a series of fictitious elastic problems. This is similar to the effective modulus approach proposed by Bažant [39] with the exception that the local force instead of the effective modulus is updated in each analysis step.

Step G: System update

In the lattice model, the entire simulation process consists of a sequence of linear analysis steps, in which the lattice beams are assumed to be linear elastic. The comparative stress within the individual element can be computed using the Eq. When the element stress is lower than the material strength (compressive or tensile), the Boltzmann superposition is valid because the element is in an undamaged state. Once the stress exceeds the material strength, this element will be removed from the mesh system, allowing for damage initialization and propagation. Creep analysis with the inclusion of element removal mechanism is adopted in the model to simulate the creep evolution under high load level (i.e., higher than 40%-50 % material strength).

$$\sigma = \alpha_N \frac{N}{A} + \alpha_M \frac{\max(M_x, M_y)}{W} \tag{6}$$

where N and M refer to the normal force and bending moment applied to the lattice beam; W and A are the cross-section and section modulus of an element, taken as identical for all elements. Two coefficients, α_N and α_M, determine whether the normal force or bending moment plays a significant role in the element failure criterion. Consistent with our previous research [60–62], their values are taken as 1.0 and 0.05.. In each analysis step, those critical elements whose stress is higher than the material strength will be removed from the system representing a series of cracks. A group of equivalent element forces, consisting of normal force, shear force, bending moment and torque, is used to replace this removed element for stress redistribution. The system stiffness is then updated considering the broken elements. In this way, the non-linear material behavior can be simulated as a sequence of linear analysis steps.

Step H: Stop criteria

For creep analysis under various loading conditions, two stop criteria are utilized. The first one regulates the timing of each loading component. When the numerical analysis reaches the loading duration of a given step, it moves into the following step. The entire numerical analysis stops until the whole load path is applied to the mesh system.

2.4. Limitations of the model

This newly proposed method is based on linear viscoelasticity. The model relies on the superposition principle, which states that the creep response of each creep stress can be superimposed. Mathematically, the stress history can be described by a linear operator. This assumption is a useful for constitutive modeling in the solution of creep integration, making numerical models available for creep calculation. However, it is not a fundamental law of physics and is only valid approximately under certain conditions. For instance, the principle may not hold true for small special cases such as drying or variable temperature scenarios. During the fresh stage of cementitious materials, hydration and flocculation processes primarily occur. These processes result in differences in

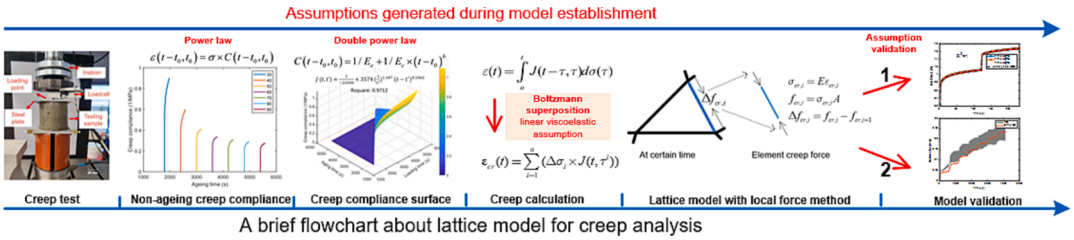

Fig. 5. A brief overview about lattice model for creep simulation.

internal structures at the meso/micro scales, which can affect time-dependent material properties such as stiffness and strength at the macro scale. Additionally, kinematic nonlinearity can also affect the creep analysis, as the creep strain can result in large deformation issues, leading to material and geometric nonlinearity. The potential nonlinear early-age creep of 3D printed materials can also impact the validity of this assumption.

However, the aim of our research is to propose a numerical method that can avoid the need for parameter fitting and there is no approximation of the creep constitutive law. Similar to other numerical methods, such as the rate-type method [36] and exponential algorithm [63], our numerical method is also based on the Boltzmann superposition principle. However, the validity of this assumption is assured by the linear viscoelasticity but also depends heavily on the tested material properties. To eliminate the impact of chemical change on early-age creep prediction, the newly proposed method takes time-dependent material stiffness as input parameters, enabling the prediction of strain history. Thus, when using experimentally derived early-age creep material properties in this numerical model, it is crucial to ensure that the chemical changes in each aging creep test can be disregarded to uphold the assumption of the Boltzmann superposition principle.

2.5. Model applicability

This newly proposed model adopts the local force method to simulate the viscosity behaviour of cementitious materials, similar to the effective elastic modulus method [37]. The model is based on the incremental algorithm and one of the main advantages is the straightforward implementation of stress history consideration. Besides, this method significantly reduces the computational cost and memory intensity since it stores just one stress parameter (i.e., element comparative stress) at each step of the analysis. In addition, the lattice model adopts the linear elastic analysis for individual steps. Once the computed stress is below material strength, there is no damage to individual elements. Thus, those lattice elements are in the elastic stage, the Boltzmann superposition for creep strain computation of each element is always valid. As a result, the lattice model with element removal technique and the incremental algorithm is valid for creep analysis of cementitious materials under high load levels.

In addition to the benefits mentioned earlier, the lattice model also has the ability to incorporate *meso*-structure. This feature allows for the consideration of material microstructure and volumetric information when converting the continuum into the lattice with beams, thus enabling the proposed method to simulate creep response with the added benefit of accounting for meso/micro structures.

3. Model validation

Fig. 5 provides an overview of the proposed numerical model, which involves model assumptions and validation. In the creep analysis, the creep compliance surface obtained from quasi-static compressive loading–unloading tests is considered as material properties, and the only fitting process is to use experimentally derived strain to calibrate the creep compliance surface. Once calibrated, no further fitting is needed, and the derived material properties serve as inputs for the computational compression test with incremental loading. The numerical result is first compared with the analytical solution derived from Boltzmann superposition to theoretically validate validity of the 'local force' method. Subsequently, the numerical results are compared with experimental findings for model validation, which can confirm the Boltzmann superposition's effectiveness in describing early-age creep. If the local force method is incorrect or significant errors arise due to the linear

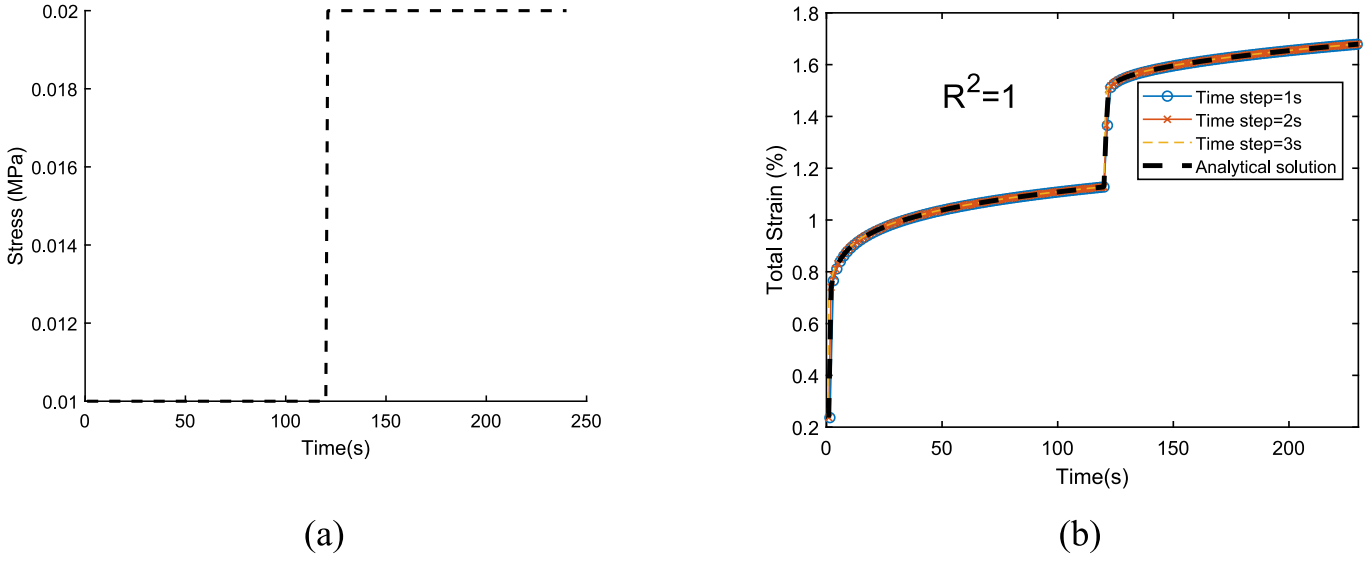

Fig. 6. Creep analysis on incremental compressive load (a) load path (b) structural strain.

Table 1
Compositions of 3D printable materials utilized in this study [kg/m^3].

Cement	Water	VMA	Sand (0.01–0.02 mm)	w/c ratio	Cement type
1140	342	0.83	770	0.3	CEM I 42.5

viscoelastic assumption, the model validation process would show significant discrepancies.

3.1. Comparison with the analytical solution

In this section, the predicted results from the lattice model are compared with the analytical solution. In addition, mesh sensitivity analysis of step size is carried out to investigate its influence on deformation prediction. The model dimension is 100 by 100 mm with a mesh resolution of 1 mm. Each load step must be independent; damage is therefore not considered in this numerical case study. Three different step sizes, namely, 1 s, 2 s, and 3 s, are used for the sensitivity analysis. Eq. (7) describes the input creep function. The initial ageing time is set to 100 s. The load path includes two parts, as shown in Fig. 6 (a).

$$J(t-\tau_i,\tau_i) = 1/4.2254 + 59.75 \times 1/\tau_i^{1.055} \times (t-\tau_i)^{0.1193} \quad (7)$$

Fig. 6 (b) shows a comparison between the analytical solution and the predicted results using lattice model with different step sizes. It can be concluded that all of them reproduce the analytical solution quantitatively, namely $R^2 = 1$. It means this newly proposed model can account for the impact of stress history and accurately describe the creep behaviour of cementitious materials.

3.2. Early-age creep test of 3D printable mortar

A series of non-ageing creep tests, in the range of 30 to 90 min after material casting, are used to validate the model application on creep evolution under constant loading. Subsequently, a compressive test which mimics the loading condition during the printing process is adopted for model validation. The material mix design can be found in Table 1. Details are provided in our previous work [47].

3.2.1. Non-ageing creep tests

Our previous research presented a repeated minutes-long creep test to characterize the early-age creep evolution of 3D printable mortar at multiple ages equal to 30, 40, 50, 60, 70, 80 and 90 min [47]. This experimental campaign consists of quasi-static loading and unloading procedures as well as 180 s loading duration between them. A sample with a diameter of 70 mm and a height of 70 mm is subjected to a compressive force of 5 N with high friction boundary condition, as shown in Fig. 3 (a). Detailed information about the sample preparation and testing process can be found elsewhere [47].

Here, the power-law function is assumed and directly adopted to fit the creep evolution of experimental findings for 3D printable materials. The creep compliance function can therefore be expressed as:

$$J(t-\tau_0,\tau_0) = 1/E_e(\tau_0) + 1/E_c(\tau_0)(t-\tau_0)^{\beta} \quad (8)$$

Here, E_e and E_c refer to the elastic and creep modulus of all lattice beams; β is the creep exponent, which stands for the impact of loading duration on creep evolution, and is determined by fitting the experimental data obtained from non-aging creep tests to a power law function. Specifically, the value of β is obtained through a curve-fitting procedure using the average experimental data. More information about this procedure can be found in the literature [3 47]. The fitted power-law expressions are then introduced into the lattice model as inputs for creep strain computation of beam elements.

The 3D numerical model is built with a mesh size of 3 mm, which consists of 10,255 lattice nodes connected by 74,195 Timoshenko beams. The radial deformation at the top and bottom sides are fixed to mimic the high friction boundary present in the test. The analyzed object is subjected to the uniaxial compressive force of 5 N. Fig. 7 (b) gives the schematic diagram of the numerical model for creep analysis.

Modelling results are then compared with experimental findings. Fig. 8 shows the comparisons between the experimental results and numerical predictions. It can be illustrated that lattice modelling of the early-age creep is in good agreement with experimental data. This demonstrates the feasibility of lattice model on non-ageing creep evolution of cementitious materials in the fresh stage.

3.2.2. Ageing creep test

In this section, the uniaxial compression tests with incrementally increased load are employed for model validation. Such tests can mimic the loading situation that occurs during the printing process. In contrast to the previous non-ageing creep test, both the loading duration and hardening time determine the creep evolution. The creep strain of lattice element is therefore computed using a double power-law expression instead of a power-law function. The above-mentioned early-age creep tests at various mortar ages are used to fit this creep function (given in Eq.). To describe the time-dependent material stiffness, the elastic modulus of lattice elements grows linearly with hardening time within 90 mins as experimental findings. This ageing creep test can be taken as a series of non-ageing creep test with the interval time equal to 10 mins. Fig. 9 shows the model input parameters, including the time-dependent material stiffness as well as the double power-law function. The applied

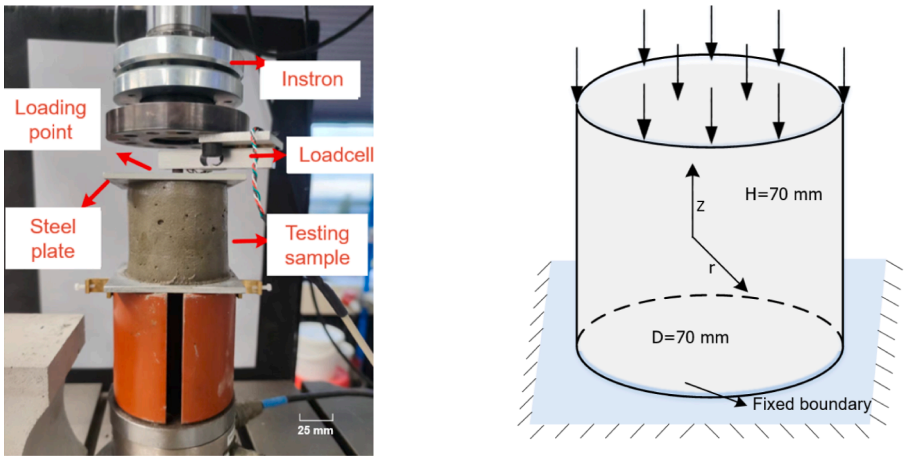

(a) (b)

Fig. 7. Early-age creep test of 3D printable mortar (a) Experimental sample [47] (b) Numerical model.

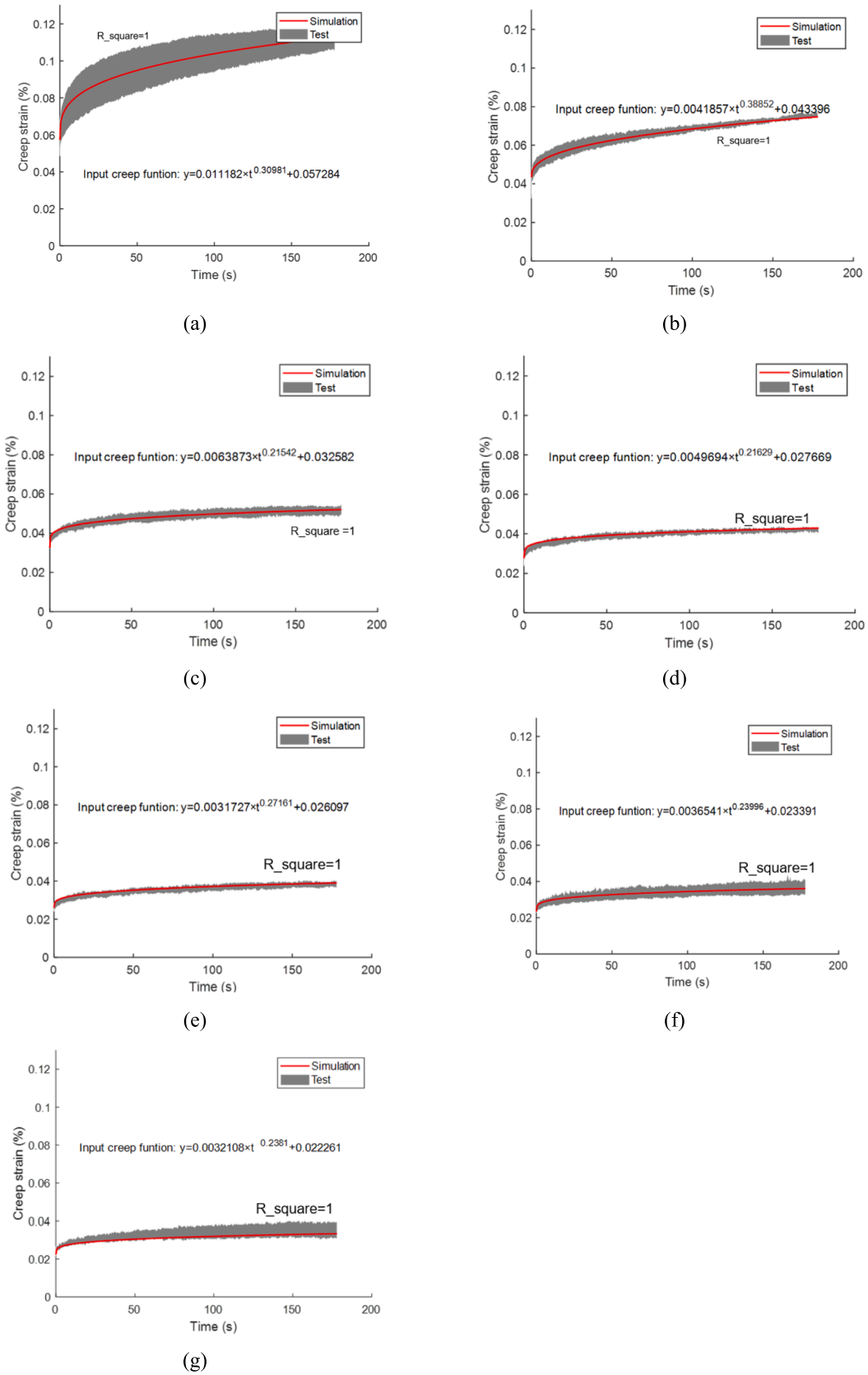

Fig. 8. The comparison between experimental findings and numerical results on early-age creep evolution at multiple mortar ages [R^2 means the difference between the average experimental data and the numerical results; for all non-ageing time creep tests, the $R^2 = 1$]. (a) 30 min (b) 40 min (c) 50 min (d) 60 min (e) 70 min (f) 80 min (g) 90 min.

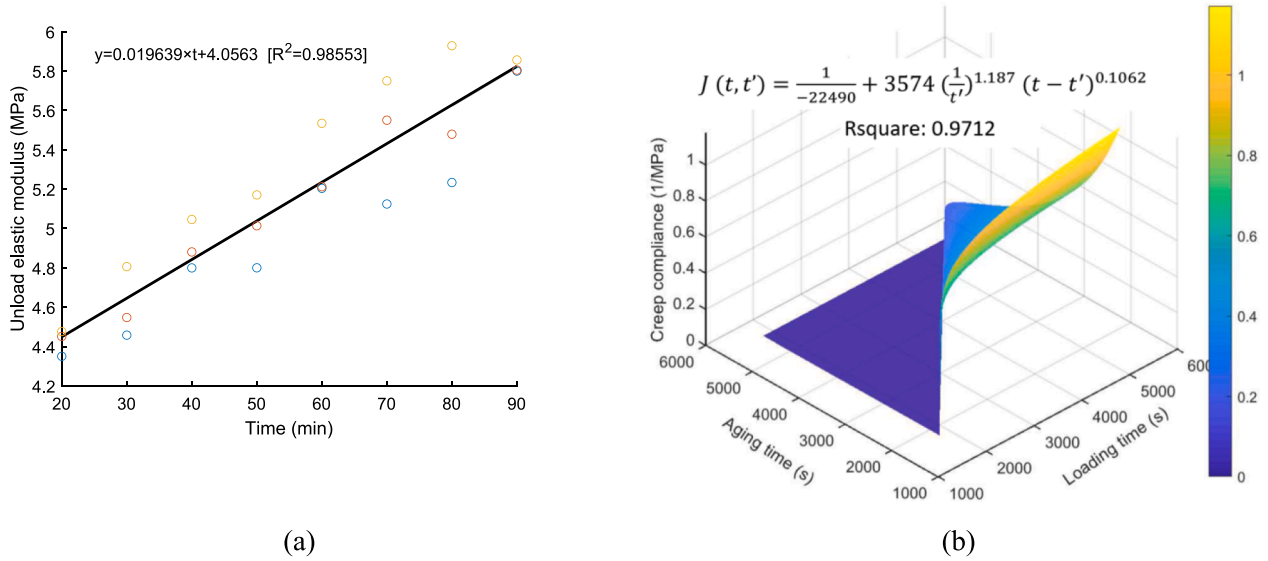

Fig. 9. Determination of input parameters for creep analysis (a) time-dependent elastic modulus (b) creep compliance [47].

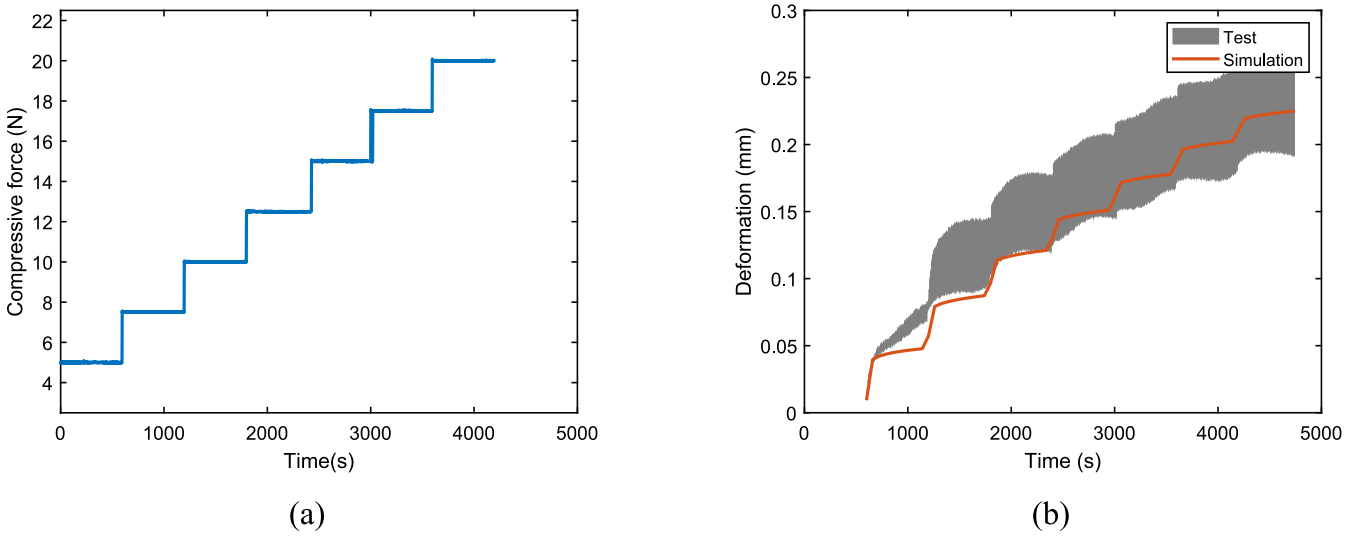

Fig. 10. Compressive creep test with incremental loading (a) loading path (b) structural deformation (Noted that the time 0 in the figures refers to the mortar age of t = 20 min).

load path can be found in Fig. 10 (a). Herein, the cylindrical sample is the same dimension as the one used in the earlier creep test.

Fig. 10 (b) shows a comparison between the simulation and experiments in relation to the creep deformation subjected to incremental compressive loading. It can be observed that the numerical simulation results show lower deformation than the experimental results in the early stage of the compression test. This might be due to the presence of internal air pores in the sample. During the initial loading, these air pores may get compressed, leading to a variation in the creep evolution and causing the experimental results to appear larger. In contrast, the numerical analysis does not consider the effect of internal air pores. However, as the loading continues and the air pores are compressed, the material properties of the matrix play a dominant influence on creep evolution of the tested sample. Lattice modelling of early-age creep evolution can reproduce the experimental results. This quantitative agreement suggests that this newly proposed model correctly considers effect of time-dependent material properties and the stress history, thereby producing a similar early-age creep deformation with the actual test.

4. Discussion

The presented numerical analyses show that this model can account for the stress history and simulate the creep behaviour of cementitious materials from fresh to hardened stages. In this section, the impact of hardening time and loading duration on creep analysis will be quantified through a series of numerical simulations. Subsequently, the early-age deformation of printed segments will be modelled to study the effect of creep on the prediction of structural deformation.

4.1. Hardening time and loading duration

In 3DCP, a specific printed segment may experience different loading situations during the printing process (namely, constant, unloading and loading situations). During the loading period, the hardening time and loading duration determine the creep evolution. When it comes to the unloading process, the creep recovery plays a significant role in predicting the structural response and understanding the mechanism of creep behaviour.

Table 2
Parametric analyses of early-age creep with different loading duration and hardening times.

Case	Applied force (N)	Hardening time (s)	Loading duration (s)	Unload force (N)
1	5	1800	300	0.5
2	5	1800	600	0.5
3	5	1800	900	0.5
4	5	180	600	0.5
5	5	18,000	600	0.5

In this section, a 3D numerical model with a diameter of 70 mm and a height of 70 mm is built. A mesh size equal to 3 mm is adopted. The whole model consists of 10,255 lattice nodes connected by 74,195 Timoshenko beams. The step size is set to 6 s in these analyses. Detailed information about these numerical analyses can be found in Table 2. A constant elastic modulus is used in these analyses to ensure the single variable analysis. A loading–unloading process is utilized to explore the model feasibility to simulate the creep recovery and investigate the impact of time (hardening time and loading duration) on creep analyses. The creep compliance is mathematically described as:

$$J(t-\tau_i,\tau_i) = 1\Big/4.6453 + 23260 \times 1\Big/\tau_i^{1.363} \times (t-\tau_i)^{0.1167} \quad (9)$$

Development of strain with different input parameters is shown in Fig. 11. Both the loading duration and hardening time affect the creep evolution. When the loading duration increases to three times, the final strain of analyzed sample increases from 0.1814% to 0.2027%. The final system strain with 180 s of hardening time is more than 100 times greater than that with 18,000 s of hardening time, indicating that the hardening time has a greater impact on creep evolution than the loading duration. In addition, the elastic and creep recovery can be observed during the unloading process, which demonstrates that the proposed model is able to simulate the creep recovery in cementitious materials.

4.2. Creep analysis of a 3D printed segment

During the printing process, cementitious materials are extruded from the nozzle and placed on the deformed geometry of an already

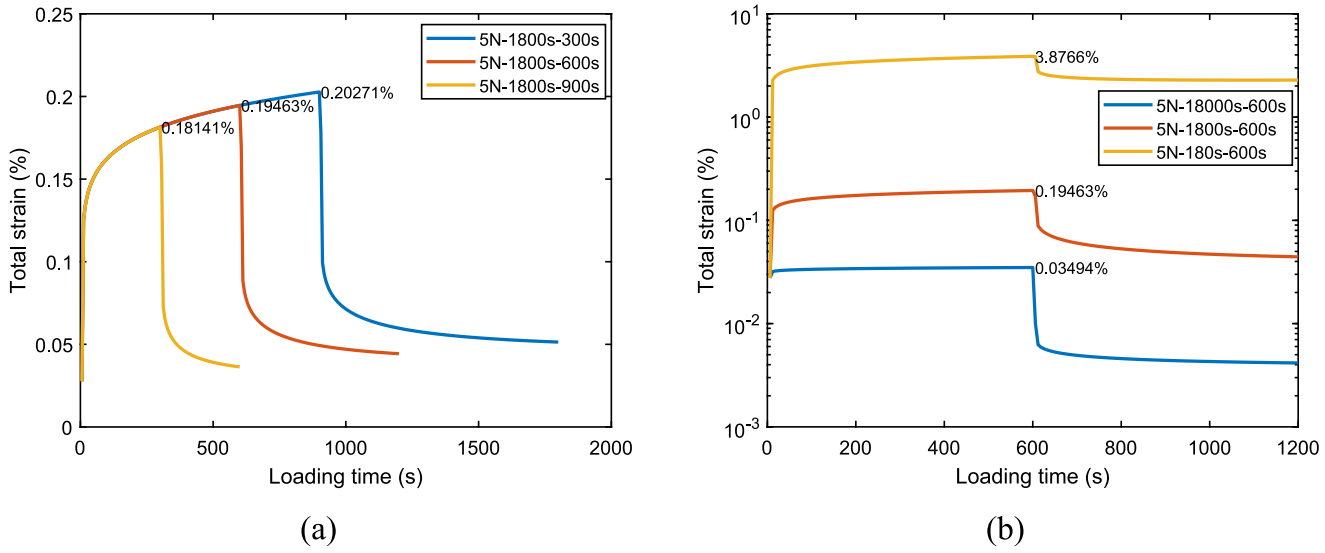

Fig. 11. Lattice modelling the creep evolution with various hardening time and loading duration (a) loading duration (b) hardening time.

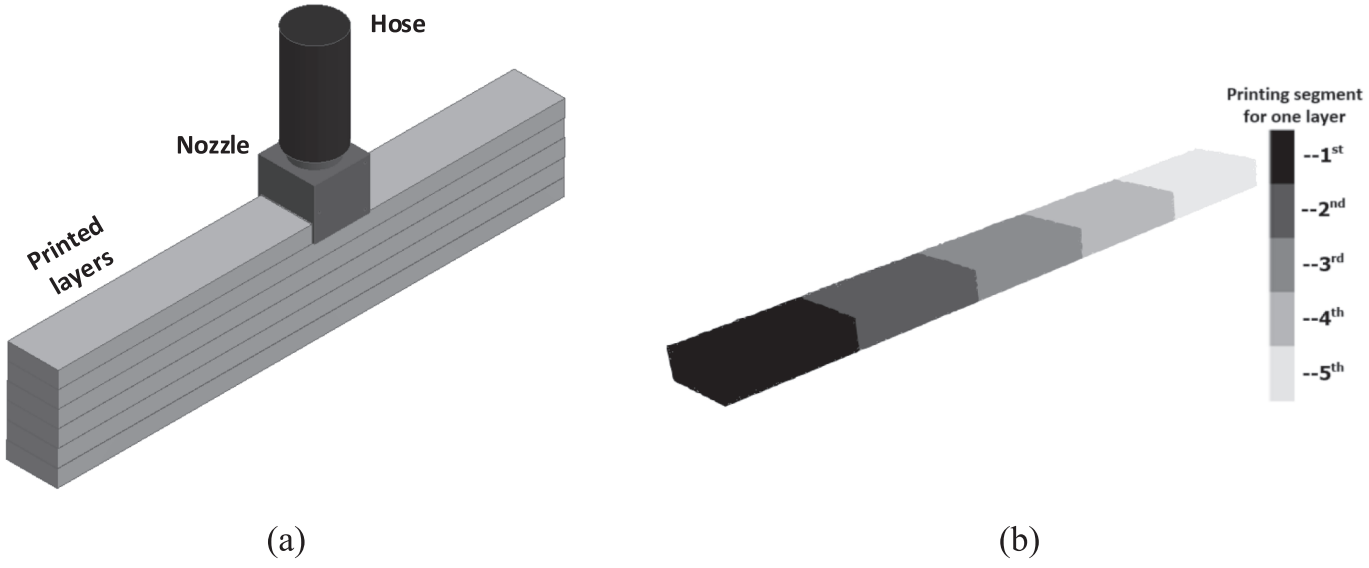

Fig. 12. Schematic of printing process (a) entire printing process (b) one specific printed segment within one printing layer.

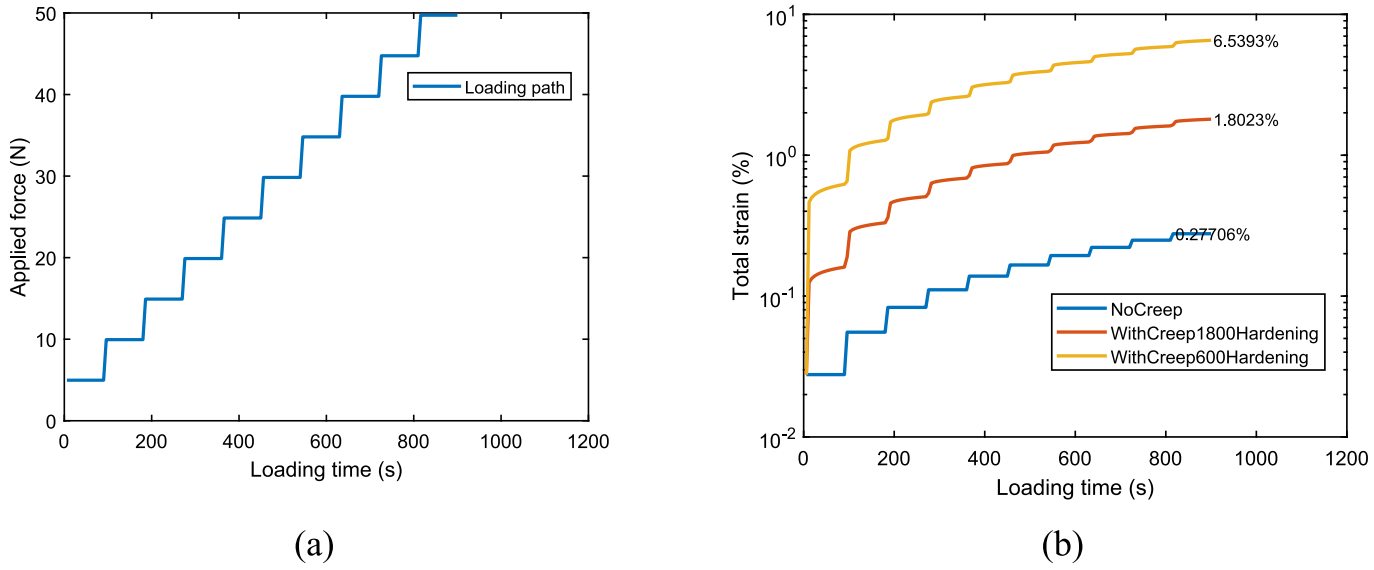

Fig. 13. Numerical analysis the deformation development of one specific printed segment (a) loading path (b) structural deformation.

printed piece, as described in Fig. 12. The compressive force from the subsequent printing layers is applied to one specific printed segment. Together with the self-weight, these forces determine the structural deformation, which includes the elastic, plastic, and time-dependent deformation.

The influence of early-age creep on structural viscoelastic deformation is studied in this section. The same model is used as in the previous section, and the creep compliance described in Eq. (9) is used. Elastic modulus is also taken as constant in the simulations. This excludes the effect of time-dependent stiffness and ensures the single variable analysis of creep on structural deformation. Fig. 13 (a) describes the loading path of this printed segment and Fig. 12 (b) demonstrates the structural deformation with or without the inclusion of creep. It should be noted that the red and orange curves refer to the creep evolution with different ageing times (namely, 600 s and 1800 s). It can be found that the structural deformation with the consideration of creep increases significantly compared to that not considering creep. In particular, the model strain with the ageing time equal to 600 s is more than 20 times larger than the one without creep. This discrepancy demonstrates the necessity of considering creep for predicting the deformation of a printed system. In the further research, early-age creep will be incorporated into the 3DCP model for buildability quantitation to study its impact on the structural analysis.

5. Conclusions

A new numerical method was proposed herein to analyse the early-age creep of 3D printable mortar. The creep compliance surface and time-dependent material behaviours obtained from previous research were taken as input parameters. This developed model was then validated through a creep test with incremental compressive loading. Based on the presented results, the following conclusions can be drawn:

- The local force method is suitable for simulating the viscoelastic behavior of cementitious materials. One of the main advantages of this approach is the straightforward implementation of stress history. This solution method requires no approximation of the creep constitutive law and produces the exact solution with the analytical model;
- The superposition principle is incorporated into the lattice model based on the incremental algorithm. The entire simulation of creep includes a sequence of linear analyses. Results of lattice analyses of the early-age creep are in good agreement with experimental results. This demonstrates the model's ability for creep analysis of 3D printable mortar under incremental/constant compressive loading;
- When predicting structural deformation of 3D printed concrete, hardening time has a greater influence on the determination of creep development than loading duration. In comparison to the model which does not consider early-age creep, the numerical result shows a very different result on the prediction of structure deformation. This discrepancy highlights the necessity of creep for the accurate prediction of viscoelasticity deformation for 3D printing concrete.

The numerical simulations in this study show that this newly proposed model can account for stress history and simulate the creep behaviour of cementitious materials from fresh to hardened stages under various loading conditions (namely, loading, unloading, and constant load). In further research, this approach will be incorporated into numerical models for 3DCP to study the impact of early-age creep on structural analysis during the printing process. Views and opinions expressed are however those of the author(s) only and do not necessarily reflect those of the European Union or the European Research Council. Neither the European Union nor the granting authority can be held responsible for them.

Declaration of Competing Interest

The authors declare that they have no known competing financial interests or personal relationships that could have appeared to influence the work reported in this paper.

Data availability

Data will be made available on request.

Acknowledgements

Ze Chang and Minfei Liang would like to acknowledge the funding supported by China Scholarship Council under grant numbers 201806060129 and 202007000027. Branko Šavija acknowledges the financial support of the European Research Council (ERC) within the framework of the ERC Starting Grant Project "Auxetic Cementitious Composites by 3D printing (ACC-3D)", Grant Agreement Number 101041342. In addition, Ze Chang wants to the thank, in partucular,

patience, accompany and support from Lu Cheng in his life. Will you marry me?

References

[1] F. Bos, R. Wolfs, Z. Ahmed, T. Salet, Additive manufacturing of concrete in construction: potentials and challenges of 3D concrete printing, Virtual Phys. Prototyping 11 (3) (2016) 209–225.
[2] R.A. Buswell, W.L. de Silva, S. Jones, J. Dirrenberger, 3D printing using concrete extrusion: A roadmap for research, Cem. Concr. Res. 112 (2018) 37–49.
[3] M. Irfan-ul-Hassan, B. Pichler, R. Reihsner, C. Hellmich, Elastic and creep properties of young cement paste, as determined from hourly repeated minute-long quasi-static tests, Cem. Concr. Res. 82 (2016) 36–49.
[4] M. Liang, Y. Gan, Z. Chang, Z. Wan, E. Schlangen, B. Šavija, Microstructure-informed deep convolutional neural network for predicting short-term creep modulus of cement paste, Cem. Concr. Res. 152 (2022), 106681.
[5] N. Ranaivomanana, S. Multon, A. Turatsinze, Tensile, compressive and flexural basic creep of concrete at different stress levels, Cem. Concr. Res. 52 (2013) 1–10.
[6] Q. Zhang, R. Le Roy, M. Vandamme, B. Zuber, Long-term creep properties of cementitious materials: Comparing microindentation testing with macroscopic uniaxial compressive testing, Cem. Concr. Res. 58 (2014) 89–98.
[7] D. Asprone, F. Auricchio, C. Menna, V. Mercuri, 3D printing of reinforced concrete elements: Technology and design approach, Constr. Build. Mater. 165 (2018) 218–231.
[8] M.S. Khan, F. Sanchez, H. Zhou, 3-D printing of concrete: Beyond horizons, Cem. Concr. Res. 133 (2020) 106070.
[9] Y. Chen, S.C. Figueiredo, Z. Li, Z. Chang, K. Jansen, O. Çopuroğlu, E. Schlangen, Improving printability of limestone-calcined clay-based cementitious materials by using viscosity-modifying admixture, Cem. Concr. Res. 132 (2020), 106040.
[10] Y. Chen, Z. Chang, S. He, O. Çopuroğlu, B. Šavija, E. Schlangen, Effect of curing methods during a long time gap between two printing sessions on the interlayer bonding of 3D printed cementitious materials, Constr. Build. Mater. 332 (2022), 127394.
[11] R.F. Feldman, Mechanism of creep of hydrated Portland cement paste, Cem. Concr. Res. 2 (5) (1972) 521–540.
[12] B.T. Tamtsia, J.J. Beaudoin, Basic creep of hardened cement paste A re-examination of the role of water, Cem. Concr. Res. 30 (9) (2000) 1465–1475.
[13] B.T. Tamtsia, J.J. Beaudoin, J. Marchand, The early age short-term creep of hardening cement paste: load-induced hydration effects, Cem. Concr. Compos. 26 (5) (2004) 481–489.
[14] H. Ye, Creep mechanisms of calcium–silicate–hydrate: an overview of recent advances and challenges, International Journal of Concrete Structures Materials 9 (4) (2015) 453–462.
[15] Z.P. Bažant, Prediction of concrete creep and shrinkage: past, present and future, Nucl. Eng. Des. 203 (1) (2001) 27–38.
[16] D.-T. Nguyen, R. Alizadeh, J.J. Beaudoin, P. Pourbeik, L. Raki, Microindentation creep of monophasic calcium–silicate–hydrates, Cem. Concr. Compos. 48 (2014) 118–126.
[17] Y. Gan, C. Romero Rodriguez, H. Zhang, E. Schlangen, K. van Breugel, B. Šavija, Modeling of microstructural effects on the creep of hardened cement paste using an experimentally informed lattice model, Comput. Aided Civ. Inf. Eng. 36 (5) (2021) 560–576.
[18] F. Wittmann, P. Roelfstra, Total deformation of loaded drying concrete, Cem. Concr. Res. 10 (5) (1980) 601–610.
[19] R. Wolfs, F. Bos, T. Salet, Early age mechanical behaviour of 3D printed concrete: Numerical modelling and experimental testing, Cem. Concr. Res. 106 (2018) 103–116.
[20] R. Wolfs, F. Bos, T.J.C. Salet, Triaxial compression testing on early age concrete for numerical analysis of 3D concrete printing, Cem. Concr. Compos. 104 (2019), 103344.
[21] J. Kruger, S. Zeranka, G. van Zijl, 3D concrete printing: a lower bound analytical model for buildability performance quantification, Autom. Constr. 106 (2019), 102904.
[22] F.P. Bos, P. Kruger, S.S. Lucas, G. van Zijl, Juxtaposing fresh material characterisation methods for buildability assessment of 3D printable cementitious mortars, Cem. Concr. Compos. 120 (2021), 104024.
[23] Z. Chang, Y. Xu, Y. Chen, Y. Gan, E. Schlangen, B. Šavija, A discrete lattice model for assessment of buildability performance of 3D-printed concrete, Computer-Aided Civil Infrastructure Engineering 36 (5) (2021) 638–655.
[24] Z. Chang, H. Zhang, M. Liang, E. Schlangen, B. Šavija, Numerical simulation of elastic buckling in 3D concrete printing using the lattice model with geometric nonlinearity, Autom. Constr. 142 (2022), 104485.
[25] A.S. Suiker, R.J. Wolfs, S.M. Lucas, T.A. Salet, Elastic buckling and plastic collapse during 3D concrete printing, Cem. Concr. Res. 135 (2020), 106016.
[26] A.S.J. Suiker, Mechanical performance of wall structures in 3D printing processes: Theory, design tools and experiments, Int. J. Mech. Sci. 137 (2018) 145–170.
[27] L. Esposito, L. Casagrande, C. Menna, D. Asprone, F. Auricchio, Early-age creep behaviour of 3D printable mortars: Experimental characterisation and analytical modelling, Mater. Struct. 54 (6) (2021) 1–16.
[28] M. Chen, B. Liu, L. Li, L. Cao, Y. Huang, S. Wang, P. Zhao, L. Lu, X. Cheng, Rheological parameters, thixotropy and creep of 3D-printed calcium sulfoaluminate cement composites modified by bentonite, Compos. B Eng. 186 (2020), 107821.
[29] Y. Mortada, M. Mohammad, B. Mansoor, Z. Grasley, E. Masad, Development of Test Methods to Evaluate the Printability of Concrete Materials for Additive Manufacturing, Materials 15 (18) (2022) 6486.
[30] R. De Borst, Smeared cracking, plasticity, creep, and thermal loading—A unified approach, Comput. Methods Appl. Mech. Eng. 62 (1) (1987) 89–110.
[31] S. Murakami, Y. Liu, M. Mizuno, Computational methods for creep fracture analysis by damage mechanics, Comput. Methods Appl. Mech. Eng. 183 (1–2) (2000) 15–33.
[32] H. Alberg, D. Berglund, Comparison of plastic, viscoplastic, and creep models when modelling welding and stress relief heat treatment, Comput. Methods Appl. Mech. Eng. 192 (49–50) (2003) 5189–5208.
[33] X. Li, Z. Grasley, E.J. Garboczi, J.W. Bullard, Modeling the apparent and intrinsic viscoelastic relaxation of hydrating cement paste, Cem. Concr. Compos. 55 (2015) 322–330.
[34] B. Han, H.-B. Xie, L. Zhu, P. Jiang, Nonlinear model for early age creep of concrete under compression strains, Constr. Build. Mater. 147 (2017) 203–211.
[35] G. Di Luzio, L. Cedolin, C. Beltrami, Tridimensional long-term finite element analysis of reinforced concrete structures with rate-type creep approach, Appl. Sci. 10 (14) (2020) 4772.
[36] S.-G. Kim, Y.-S. Park, Y.-H. Lee, Rate-type age-dependent constitutive formulation of concrete loaded at an early age, Materials 12 (3) (2019) 514.
[37] Z.P. Bazant, R. L'Hermite, Mathematical modeling of creep and shrinkage of concrete, (1988).
[38] P. Gao, G. Ye, H. Huang, Z. Qian, E. Schlangen, J. Wei, Q. Yu, Incorporating elastic and creep deformations in modelling the three-dimensional autogenous shrinkage of cement paste, Cem. Concr. Res. 160 (2022), 106907.
[39] Z.P. Bazant, Prediction of concrete creep effects using age-adjusted effective, J. Am. Concr. Inst 69 (4) (1972) 212–217.
[40] K. Kovler, Drying creep of concrete in terms of the age-adjusted effective modulus method, Mag. Concr. Res. 49 (181) (1997) 345–351.
[41] Z. Cheng, R. Zhao, Y. Yuan, F. Li, A. Castel, T. Xu, Ageing coefficient for early age tensile creep of blended slag and low calcium fly ash geopolymer concrete, Constr. Build. Mater. 262 (2020), 119855.
[42] Y.-S. Park, Y.-H. Lee, Y. Lee, Description of concrete creep under time-varying stress using parallel creep curve, Adv. Mater. Sci. Eng. 2016 (2016) 1–13.
[43] M.A. Pisani, Behaviour under long-term loading of externally prestressed concrete beams, Eng. Struct. 160 (2018) 24–33.
[44] Z.P. Bažant, S. Prasannan, Solidification theory for concrete creep. II: Verification and application, J. Eng. Mech. 115 (8) (1989) 1704–1725.
[45] C. Européen, Eurocode 2: Design of concrete structures—Part 1–1: General rules and rules for buildings, British Standard Institution, London, 2004.
[46] A.C.J.A. R-08, Guide for modeling and calculating shrinkage and creep in hardened concrete, American Concrete Institute Farmington Hills, MI, 2008.
[47] Z.e. Chang, M. Liang, Y. Xu, Z. Wan, E. Schlangen, B. Šavija, Early-age creep of 3D printable mortar: experiments and analytical modelling, Cem. Concr. Compos. 138 (2023) 104973.
[48] P. Rossi, J.-L. Tailhan, F. Le Maou, L. Gaillet, E. Martin, Basic creep behavior of concretes investigation of the physical mechanisms by using acoustic emission, Cem. Concr. Res. 42 (1) (2012) 61–73.
[49] M.F. Ruiz, A. Muttoni, P.G. Gambarova, Relationship between nonlinear creep and cracking of concrete under uniaxial compression, J. Adv. Concr. Technol. 5 (3) (2007) 383–393.
[50] Z.P. Bažant, B.H. Oh, Crack band theory for fracture of concrete, Matériaux et construction 16 (3) (1983) 22.
[51] H.J. Herrmann, A. Hansen, S. Roux, Fracture of disordered, elastic lattices in two dimensions, Phys. Rev. B 39 (1) (1989) 637–648.
[52] E. Schlangen, E.J. Garboczi, Fracture simulations of concrete using lattice models: computational aspects, Eng. Fract. Mech. 57 (2–3) (1997) 319–332.
[53] J.E. Bolander, N. Sukumar, Irregular lattice model for quasistatic crack propagation, Phys. Rev. B 71 (9) (2005), 094106.
[54] P. Grassl, A lattice approach to model flow in cracked concrete, Cem. Concr. Compos. 31 (7) (2009) 454–460.
[55] B. Šavija, J. Pacheco, E. Schlangen, Lattice modeling of chloride diffusion in sound and cracked concrete, Cem. Concr. Compos. 42 (2013) 30–40.
[56] B. Šavija, M. Luković, J. Pacheco, E. Schlangen, Cracking of the concrete cover due to reinforcement corrosion: A two-dimensional lattice model study, Constr. Build. Mater. 44 (2013) 626–638.
[57] M. Luković, B. Šavija, E. Schlangen, G. Ye, K. van Breugel, A 3D Lattice Modelling Study of Drying Shrinkage Damage in Concrete Repair Systems, Materials (Basel) 9 (7) (2016) 575.
[58] P. Gao, Y. Chen, H. Huang, Z. Qian, E. Schlangen, J. Wei, Q. Yu, Investigation of drying-induced non-uniform deformation, stress, and micro-crack propagation in concrete, Cem. Concr. Compos. 114 (2020), 103786.
[59] E. Schlangen, O. Çopuroglu, Concrete damage due to alkali-silica reaction: A new method to determine the properties of expansive gel, Fracture mechanics of concrete and concrete structures–high-performance concrete, brick-masonry and environmental aspects, Taylor & Francis Group, London, 2007, pp. 1835–1841.
[60] H. Zhang, Y. Xu, Y. Gan, Z. Chang, E. Schlangen, B.J.C. Šavija, C. Research, Combined experimental and numerical study of uniaxial compression failure of hardened cement paste at micrometre length scale, Cem. Concr. Res. 126 (2019), 105925.

[61] N. Jiang, H. Zhang, Z. Chang, E. Schlangen, Z. Ge, B. Šavija, Discrete lattice fracture modelling of hydrated cement paste under uniaxial compression at micro-scale, Constr. Build. Mater. 263 (2020), 120153.
[62] Z. Chang, H. Zhang, E. Schlangen, B. Šavija, Lattice Fracture Model for Concrete Fracture Revisited: Calibration and Validation, Appl. Sci. 10 (14) (2020) 4822.
[63] Z.P. Bažant, J.-C. Chern, Strain softening with creep and exponential algorithm, J. Eng. Mech. 111 (3) (1985) 391–415.